Three-Dimensional Flow Analysis and Improvement of Slip Factor Model for Forward-Curved Blades Centrifugal Fan

En-Min GUO, Kwang-Yong KIM*
Department of Mechanical Engineering, Inha University
Incheon 402-751, Korea

This work developed improved slip factor model and correction method to predict flow through impeller in forward-curved centrifugal fan. Both steady and unsteady three-dimensional CFD analyses were performed to validate the slip factor model and the correction method. The results show that the improved slip factor model presented in this paper could provide more accurate predictions for forward-curved centrifugal impeller than the other slip factor models since the present model takes into account the effect of blade curvature. The correction method is provided to predict mass-averaged absolute circumferential velocity at the exit of impeller by taking account of blockage effects induced by the large-scale backflow near the front plate and flow separation within blade passage. The comparison with CFD results also shows that the improved slip factor model coupled with the present correction method provides accurate predictions for mass-averaged absolute circumferential velocity at the exit of impeller near and above the flow rate of peak total pressure coefficient.

Key Words : Forward-Curved Blades Centrifugal Fan, Slip Factor, Three-Dimensional CFD, Blade Curvature, Blockage Effect

Nomenclature

a : Effective passage width
b : Blade width
B_F : Blockage coefficient due to backflow near the front plate
B_S : Blockage coefficient due to flow separation from suction surface
C_r, C_u, C_z : Absolute velocity component in radial, circumferential, axial direction, respectively
C_m : Meridional velocity (nearly equal to C_r at the exit of impeller)
D : Diameter
n : Perpendicular direction to flow
p : Static pressure
p_t : Total pressure
Q : Volume flow rate
R : Radius
R_b : Radius of curvature of blade
R_v : Radius of scroll (as shown in Figure 1)
s : Flow direction
t : Blade thickness
T : Wake width
U : Peripheral speed
w : Relative velocity
W : Scroll width
z : Blade number
α_v : Scroll angle
θ_c : Cutoff angle (as shown in Figure 1)
θ_v : Scroll angle from the origin (as shown in Figure 1)
β : Blade angle
δ : Opening angle of blade camber at the exit
ε : Total blockage coefficient
γ : Flow deflection angle in the discharge stream of blade
φ : Flow coefficient $(=Q/\pi b_2 D_2 U_2)$
μ : Slip factor $(=C'_{u2}/C_{u2})$

* Corresponding Author,
E-mail : kykim@inha.ac.kr
TEL : +82-32-872-3096; **FAX** : +82-32-868-1716
Department of Mechanical Engineering, Inha University Incheon 402-751, Korea. (Manuscript **Received** May 6, 2003; **Revised** October 18, 2003)

ρ : Flow density
ω : Rotating speed
ψ : Total pressure coefficient $(=\Delta p_t/\rho U_2^2)$

Subscripts
1, 2: Impeller inlet, outlet or blade tip

Superscripts
$\overline{(\ )}$: Area-averaged quantity
$\overline{(\ )}$: Mass-averaged quantity
(Prime values denote actual flow angle and velocity with slip considered)

1. Introduction

Forward-curved blades or squirrel-cage centrifugal fans are widely used in air-conditioning and ventilating systems, due to the characteristics of relatively low noise and high flow rate. As shown in Fig. 1, their main components are forward-curved centrifugal impeller and scroll. The distinguished features of this kind of fans are the large inlet-to-exit diameter ratio of over 0.8, large width to diameter ratio of over 0.25, short and simple forward-curved shape of blade (usually with camber of single or double arc shape, and constant thickness of sheet metal), and a large number of blades for impeller.

The flow through this type of impeller is quite complex due to unsteady and asymmetric flow through the impeller, interaction between the impeller and the scroll, and especially large scale backflow through the impeller near the front plate, as calculated by Seo et al.(2003), shown in Fig. 2. Consequently, peak efficiency of the impeller is only about 60 percent, and the total efficiency is up to 30 or 40 percent.

As any other centrifugal fans, the design of this fan usually begins with a one-dimensional vector diagram analysis. In this design process, key geometric parameters, for example, inlet and exit diameters, blade angles, blade width, scroll angle, cut-off clearance, etc. are optimized to achieve the high performance. This process is based on the performance analysis with various models for slip factor (Wiesner, 1967) and losses (Eck, 1973). However, some evidences show that the conventional models seldom give reasonable predictions for the performance of these fans due to the complex flowfield as already discussed. Kim and Kang (1997) showed that measured slip factors do not agree with conventional slip factor models at most of flow rate range. Therefore, it is not expected to predict the performance correctly with these models.

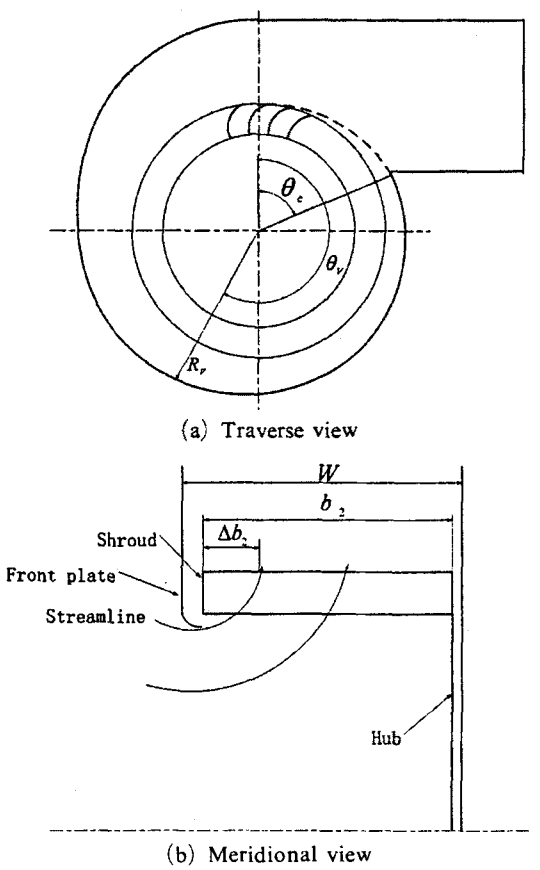

Fig. 1 Configuration of forward-curved blades fan

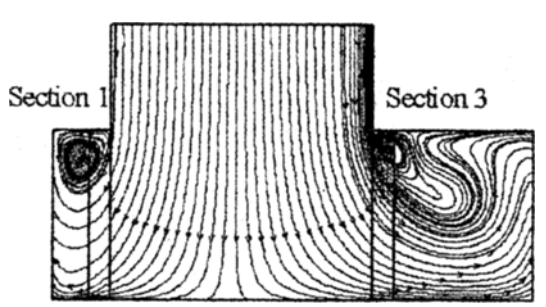

Fig. 2 Calculated Streamlines obtained by Seo, et al. (2003)

Yamazaki (1986, 1987a, 1987b) developed slip factor model and loss models for special application to forward-curved blades centrifugal fan based on experimental results. Unfortunately, Yamazaki's model often considerably underestimates slip factor and theoretical total pressure rise, therefore does not provide correct prediction for the performance in most of the cases. Kind (1997) suggested, for performance analysis, another kind of method, which substitutes the slip factor model by deviation angle model to evaluate velocity diagram at the exit of impeller as in the analysis of axial flow turbomachinery, and analyzes the flow in scroll by subdividing the scroll into sectors along the circumferential direction. Although the calculation process is rather complicate, it seems Kind's method reasonably predicts the performance for some of these fans. However, the assumption employed in this method, which neglects the backflow through the impeller, severely restricts its application to most of forward-curved blades centrifugal fans of large width to diameter ratio with large scale backflow, as shown in Fig. 2.

Although a lot of experimental works have been reported for this type of centrifugal fan (Kwon and Cho, 2001 ; Sandra Velarde-Suarez et al., 1999 ; Raj and Swim, 1981 ; Kind and Tobin, 1990), few of them is helpful to validate the models for slip factor and losses because detailed data about flowfield were not provided. However, the evolution of CFD (Computational Fluid Dynamics) makes it possible to have detailed insight into the flowfield in this centrifugal fan with sufficient accuracy (Thomas Bouquet et al., 2002).

In order to develop one-dimensional analysis method for forward-curved blades centrifugal fan, the present study aims at developing improved slip factor model by investigating the performance of various slip factor models, and also at providing new correction method to take account of the viscous effects. Steady and unsteady three-dimensional CFD calculations are carried out, and the performances of the slip factor models and the correction method are validated with the CFD results.

2. Three-Dimensional Flow Analysis

Both steady and unsteady three-dimensional calculations of the flowfield in forward-curved blades centrifugal fan have been carried out with a commercial Navier-Stokes code, CFX-TASC flow. Reynolds averaging is applied to the governing equations in strong conservation form for the turbulent flow. The k-ε turbulence model is employed as a turbulence closure.

The structured H-type mesh with 794,435 nodes in total is used for this calculation. The whole calculation domain of this fan is divided into three zones ; impeller, inlet, and scroll zones. In the impeller zone, 3,920 nodes (28, 14, and 10 nodes are distributed with non-uniform spaces in axial, radial, and circumferential directions, respectively) are used in each blade passage. On the interfaces of any two zones, one node per degree is specified in circumferential direction, and the same distribution of nodes in axial direction is employed at any circumferential position, so that the nodes of two zones can coincide with each other on the interface at any physical time step in the unsteady calculation. Fig. 3 shows the mesh system and the nodes distribution at the cross section of impeller.

As the boundary conditions, the flow rate is fixed at the exit of scroll, and the total pressure is given at the inlet. The inlet and impeller zones are specified in a rotating frame, but, the scroll zone is specified in a stationary frame. Therefore, the frozen rotor and rotor/stator interface conditions are specified for steady and unsteady calculations, respectively. The detailed information about these

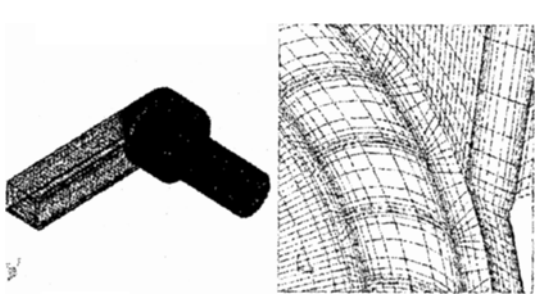

Fig. 3 Mesh system

Table 1 Geometric parameters of the fan

Impeller		Blade		Scroll	
D_1	0.1283 m	β_1	86.8°	α_v	3.4°
D_2	0.159 m	β_{22}	151.3°	W	0.111 m
b	0.1 m	t	0.5 mm	θ_c	71.6°
Z	36	Shape	Single circular arc	r_c	3.8 mm

two interface conditions can be found in CFX-TASCflow user documentation.

Specifications of the fan used in the present work are presented in Table 1. The fan tested in this work is a forward-curved blades centrifugal fan of double suction type. In order to reduce the computing time, only a half of the fan is simulated, and symmetric condition is specified at the central plane.

3. Improved Slip Factor Model

Among the slip factor models developed so far, some of them, such as proposed by Yamazaki (1987a) and Wiesner (1967), were developed based on experimental data and empirical correlations, but, the others such as proposed by Stodola (1927) and Eck (1973) were developed based on theoretical solutions of which accuracies depend on the fundamental assumptions employed in the procedures.

In Stodola model (1927), it is assumed that slip velocity is induced by the relative rotation of the flow through the passage or relative eddy within the blade passage. And, a concise expression is given to predict slip velocity as follows.

$$\Delta C_u = \frac{a}{2}\omega \tag{1}$$

where a is the effective passage width at the exit of impeller. Although this method does not take into account the effect of blade curvature, the basic idea correlating slip velocity to relative eddy within blade passage is widely accepted (Eck, 1973), and is also adopted in this work.

For forward-curved centrifugal impeller with simple blade shape (single or double arc), the relative rotation of the flow through the blade passage can be related to blade curvature by

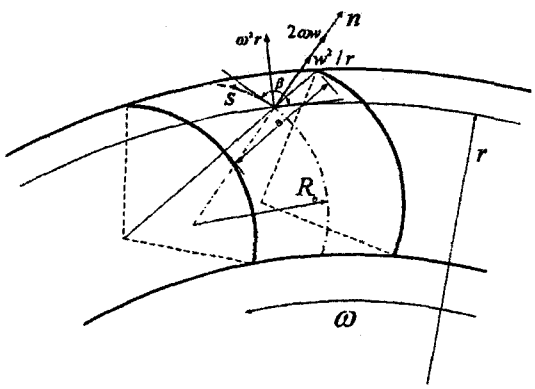

Fig. 4 Force equilibrium on fluid particle within the blade passage

considering the equilibrium condition of fluid particle within the blade passage. As shown in Fig. 4, the flow particle moves in the passage defined by blade geometry, and the momentum equations in the directions of blade radius of curvature and streamline, respectively, can be written as follow.

$$\frac{1}{\rho}\frac{\partial p}{\partial n} = \frac{w^2}{R_b} + \omega^2 r \cos\beta + 2\omega w \tag{2}$$

$$\frac{1}{\rho}\frac{\partial p}{\partial s} - w\frac{\partial w}{\partial s} + \omega^2 r \sin\beta \tag{3}$$

or

$$\begin{aligned}\frac{1}{\rho}dp &= -wdw + \omega^2 r \sin\beta ds \\ &= -wdw + \omega^2 r dr\end{aligned} \tag{4}$$

From Eq. (4), following energy equation of the relative flow can be obtained.

$$\frac{1}{\rho}p + \frac{1}{2}w^2 - \frac{1}{2}\omega^2 r^2 = const \tag{5}$$

If the friction losses are neglected, the gradient of relative velocity in the cross-streamwise direction can be obtained by combining Eqs. (2) and (5) (Eck, 1973).

$$\frac{\partial w}{\partial n}=-\left(2\omega+\frac{w}{R_b}\right) \tag{6}$$

As interpreted by Eck (1973), the relative rotation of the total flow through blade passage is equal to the linear relative velocity gradient.

$$\omega'=\left|\frac{\partial w}{\partial n}\right|=2\omega+\frac{w}{R_b} \tag{7}$$

Slip velocity is then approximately represented by the induced velocity of the average rotation, which is a half of the total rotation ω', at the center of blade passage at the exit of impeller.

$$\Delta C_{u2}=\frac{\omega'}{2}\frac{a}{2}=\frac{U_2}{D_2}a+\frac{Q}{4zb_2R_b} \tag{8}$$

Therefore, the slip factor for forward-curved centrifugal impeller can be obtained as follows.

$$\mu=\frac{C'_{u2}}{C_{u2}}=\frac{C_{u2}-\Delta C_{u2}}{C_{u2}}=1-\frac{\frac{U_2}{D_2}a+\frac{Q}{4zb_2R_b}}{U_2-\frac{Q}{\pi D_2b_2\tan\beta_2}} \tag{9}$$
$$=1-\frac{a/D_2+\varphi\pi D_2/4zR_b}{1-\varphi/\tan\beta_2}$$

The improved model for slip factor takes into account the effect of blade curvature, and thus can be expected to provide more reasonable prediction for the circumferential component of the actual absolute velocity at the exit of forward-curved centrifugal impeller.

4. Correction to Conventional Slip Factor Models

Investigation of Senoo et al.(1974) indicates that slip factor and mass-averaged velocity could be affected by the viscous effects including blockage of flow passage, variation of effective camber lines, and friction force. A lot of evidences show that the influence of blockage, due to backflow near the front plate and flow separation from suction surface of the blades, is more remarkable for forward-curved blades centrifugal fans. A correction method is accordingly suggested here to predict mass-averaged absolute circumferential velocity.

4.1 Blockage of flow passage due to backflow near the front plate

Yamazaki's blockage coefficient correlation method (1986) is employed in this work to predict the blockage coefficient, B_F due to backflow near the front plate.

$$B_F=0.38+c\left|\frac{b_2}{D_2}-0.35\right|^2 +0.62\left(\frac{D_1}{D_2}-0.86\right)+0.25(\varphi-0.3) \tag{10}$$

where

$$c=14.8,\ \text{if}\ \frac{b_2}{D_2}<0.35$$

$$c=3.0,\ \text{if}\ \frac{b_2}{D_2}\geq 0.35$$

4.2 Blockage of flow passage due to flow separation from the suction surface

For forward-curved blades centrifugal fans, Eck (1973) provides a method to determine the position where the flow separates from the suction surface of blade according to flow deflection in the discharge stream. As shown in Fig. 5, if we adopt Stodola's assumption (Stodola, 1927), i.e., the velocity gradient equal to a rotation of the total flow across blade passage, employed in the above section, the average excess velocity at the discharge area with effective passage width of a can be evaluated as follows.

$$\Delta w=\omega' a/2=\left(\omega+\frac{\bar{w}}{2R_b}\right)a \tag{11}$$

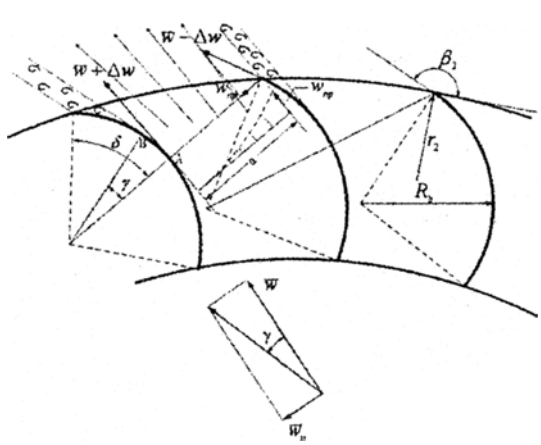

Fig. 5 Flow pattern about flow separation from suction surface

where $\bar{w}(=Q/zab_2)$ is mean velocity. Eck assumes a parabolic distribution for the reduction of velocity component in the direction perpendicular to mean flow with the smallest value of zero occurring at the end point A on suction surface, and the largest value occurring at the side of pressure surface.

$$w_{np}=(\bar{w}-\Delta w)\sin\delta$$
$$=\left[\bar{w}-\left(\omega+\frac{\bar{w}}{2R_b}\right)a\right]\sin\delta \quad (12)$$

Thus, the following average value for this velocity component is obtained.

$$\bar{w}_n=\frac{1}{3}w_{np}=\frac{1}{3}\left[\bar{w}-\left(\omega+\frac{\bar{w}}{2R_b}\right)a\right]\sin\delta \quad (13)$$

And, the flow deflection angle γ can be calculated from the average value.

$$\tan\gamma=\bar{w}_n/\bar{w}=\frac{1}{3}\left[1-\left(\frac{\omega}{\bar{w}}+\frac{1}{2R_b}\right)a\right]\sin\delta \quad (14)$$

Then, the separation point B (with the arc angle from point A of γ) on the suction surface can be determined, and the wake width T is as follows.

$$T=R_b[1-\cos(\delta-\gamma)] \quad (15)$$

Therefore, the blockage coefficient, B_S due to wake or boundary layer separation can be calculated approximately.

$$B_S=\frac{zT}{\pi D_2\cos\left[\beta_2-\frac{\pi}{2}-\delta+\gamma\right]} \quad (16)$$

As shown in Fig. 6, the correction of the circumferential component of the actual absolute velocity due to blockage effect can be obtained.

$$\Delta C'_{u2}=w'_2\cos(\pi-\beta'_2)\frac{\varepsilon}{1-\varepsilon} \quad (17)$$

where

$$\varepsilon=B_F+(1-B_F)B_S$$
$$\beta'_2=\pi-\tan^{-1}\frac{C_{m2}}{w'_{u2}}$$

Therefore, the mass-averaged absolute circumferential velocity can be expressed as follows.

$$\bar{C}_{u2}=C'_{u2}+\Delta C'_{u2} \quad (18)$$

where C'_{u2} is calculated with slip factor model.

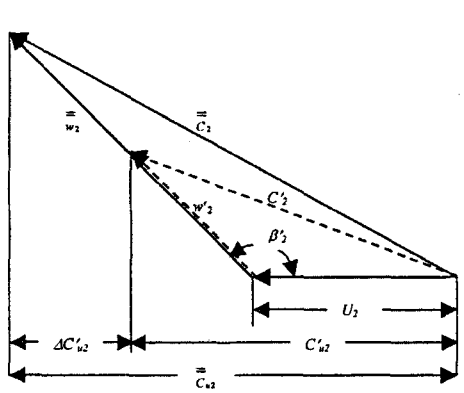

Fig. 6 Velocity triangles to indicate blockage effect

5. Results and Discussion

To validate the performance of the slip factor model developed in this work, the predictions with the present model are compared with those with the conventional models, i.e., the models proposed by Wiesner (1967), Eck (1973), Yamazaki (1987a), and Stodola (1927), as well as with CFD results.

The predictions for total pressure coefficient based on steady CFD calculation at both of the exits of impeller and scroll are shown in Fig. 7 (a). It can be found that the peak total pressure coefficient at the exit of impeller occurs at the flow coefficient $\varphi=0.265$. Although the impeller shows stable operation in the range of flow coefficient in this work, the steep total pressure coefficient curve of the whole configuration indicates the poor matching of scroll and impeller.

Figure 7(b) shows the variations of circumferential averaged slip factor with the flow coefficient predicted by steady CFD simulation, in which two methods for evaluating slip factor are employed as follows.

$$\bar{\mu}=\frac{\bar{C}_{u2}}{U_2+\bar{C}_{m2}/\tan\beta_2} \text{ for mass-weighted average}$$

$$\bar{\mu}=\frac{\bar{C}_{u2}}{U_2+\bar{C}_{m2}/\tan\beta_2} \text{ for area-weighted average}$$

It can be found that, both the mass-weighted and area-weighted circumferential-averaged slip factors decrease as the flow coefficient increase, but

level of the former is much less than that of the latter, and the variation of the former with flow coefficient is steeper. In this figure, it is also found that, in the entire range of flow rate considered in this work, all of the predictions except that with Yamazaki model are closer to area-weighted circumferential-averaged slip factor based on CFD calculations than to mass-weighted one. Although Yamazaki model was developed specially for forward-curved blades fan, it gives the worst predictions, which are considerably lower than the CFD results.

The flowfield at the middle of the impeller width shown in Fig. 8 implies huge incidence angle at the leading edge of impeller, and backflow near the front plate, which is the main reason for the difference of slip factor between predictions with conventional slip factor models and CFD results in Fig. 7.

Because steady CFD calculation with frozen rotor condition for the interface between impeller and scroll zones can not take into account the effect of unsteady interaction, steady calculation results are compared with unsteady calculation

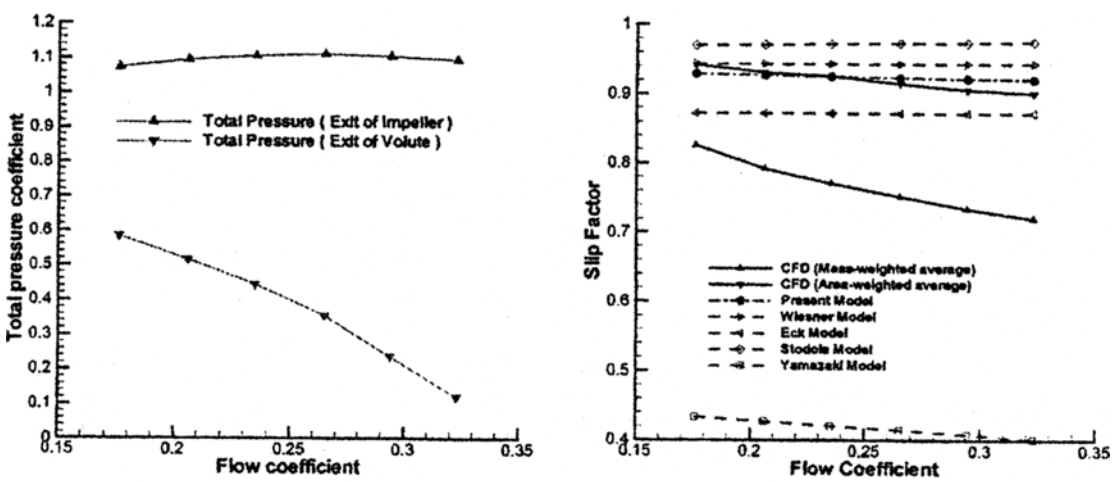

(a) Total pressure coefficient (b) Slip factor

Fig. 7 Predicted performance curves

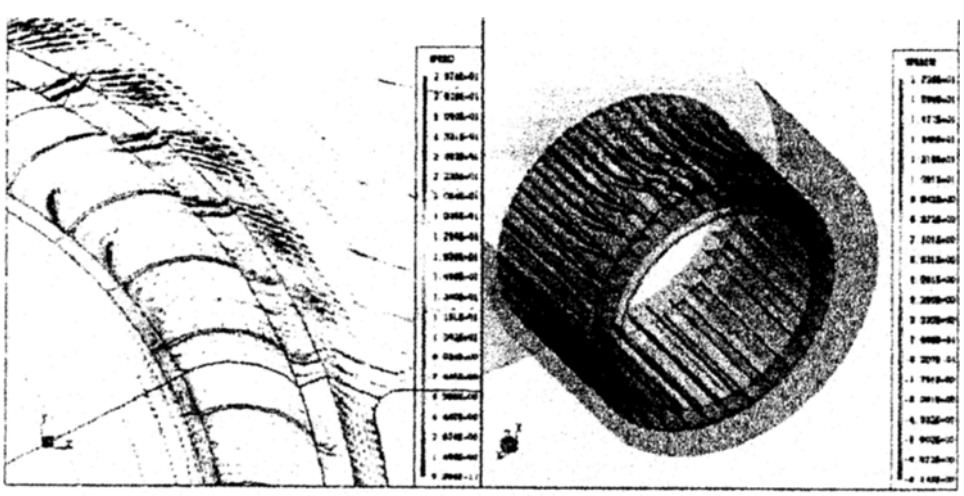

(a) Velocity vector (b) Radial velocity at the exit of impeller

Fig. 8 Flowfield through forward-curved blades impeller

results in Fig. 9 and Table 2, to evaluate the validity of steady calculations. The circumferential distributions of velocity and slip factor, which are obtained by averaging in the axial direction, shown in Fig. 9 indicate that, except in the vicinity of the volute tongue, the results with steady calculation is in good agreement with unsteady calculation results. The negligible differences in circumferential-averaged values shown in Table 2 further verify that the unsteady effects can be neglected for the evaluation of overall performance.

Because of the strong interaction between impeller and volute, it seems, from Fig. 9(b), that it is difficult to predict the circumferential distribution of slip factor correctly with conventional models even if non-uniform circumferential distribution of flow rate is taken into account. Especially, in the vicinity of the volute tongue, the slip factors larger than 1.0 cannot be interpreted with conventional slip factor models.

In the above analysis, both the methods of mass-weighted and area-weighted averages are employed to evaluate velocity based on the CFD results in order to avoid the possible confusion in comparing results of CFD with those of slip factor models. Mass-averaged value, rather than area-averaged value, for absolute circumferential velocity is important in evaluating the theoretical total pressure rise within impeller, especially for such a centrifugal fan with large scale reverse or separated flow. However, when slip factor models (except Yamazaki model) are applied to predict actual velocity at the exit of impeller, it is difficult to take account of the effect of non-uniformity in flowfield.

$$\mu=\frac{C'_{u2}}{C_{u2}}=\frac{C'_{u2}}{U_2-\dfrac{Q}{\pi D_2 b_2 \tan\beta_2}}=\frac{C'_{u2}}{U_2-\dfrac{\bar{C}_{m2}}{\tan\beta_2}} \quad (19)$$

For forward-curved blades centrifugal fan, large scale backflow or separated flow results in great difference between mass-averaged and area-averaged values for any parameter in actual flow-

Table 2 Circumferential-averaged velocity components at exit of impeller and slip factor

	Radial velocity		Absolute circumferential velocity		Slip Factor	
	$\bar{C}'_r/U_2$	$\bar{C}'_r/U_2$	$\bar{C}'_u/U_2$	$\bar{C}'_u/U_2$	$\bar{\mu}$	$\bar{\mu}$
Unsteady	0.31	0.85	1.43	1.84	0.9151	0.7213
Steady	0.31	0.83	1.42	1.85	0.9050	0.7340

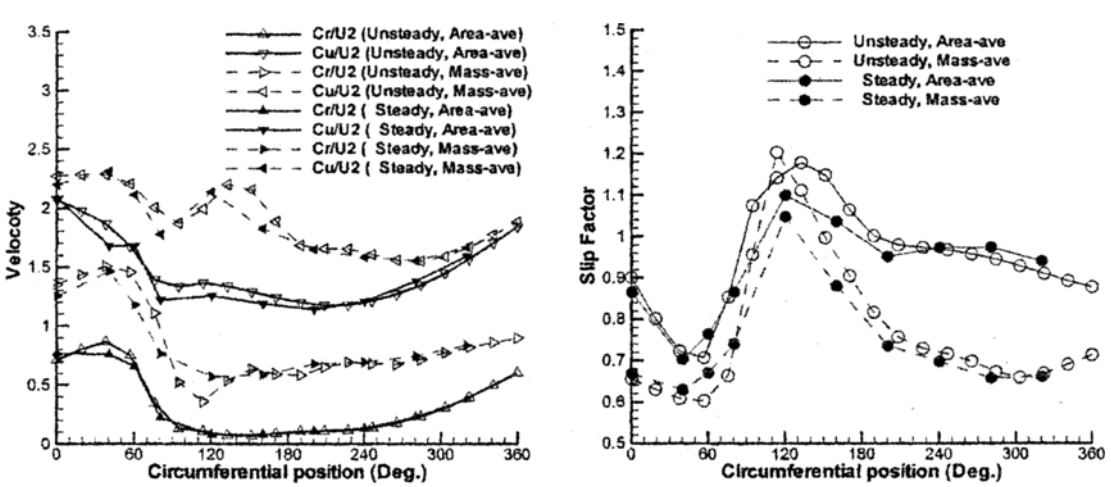

(a) Distributions of velocity at exit of impeller (b) Distributions of slip factor

Fig. 9 Comparison of steady and unsteady CFD results

field (as shown in Figs. 7 and 9, and Table 2). This is also the reason why slip factors with conventional models are closer to area-averaged value than to mass-averaged value based on CFD results.

Consequently, with actual significance and final interest, predicted circumferential components of absolute velocity with slip factor models are compared with mass-weighted and area-weighted averaged velocities based on CFD results. As shown in Fig. 10, the mass-averaged absolute circumferential velocity evaluated from CFD results is greater than area-averaged value by over 20 percent, and the discrepancy increases with the flow coefficient, which implies that the backflow within impeller becomes stronger as the flow coefficient increases. All of the predicted absolute circumferential velocities with various slip factor models are still closer to area-averaged values in entire flow rate range. Although the slip factor with Eck model is closest to mass-averaged value in Fig. 7, in this case for absolute circumferential velocity shown in Fig. 10, Eck model gives rather poor results.

It is found, in Figs. 7(b) and 10(a), that the slip factor model developed in this work predicts slip factor and absolute circumferential velocity closest to area-averaged values among the slip factor models tested in this work. Especially, at the flow rate where peak total pressure coefficient of impeller takes place (φ=0.265), predicted absolute circumferential velocity with present model agrees with area-averaged value very well. The agreement between predicted absolute circumferential velocity with present model and the area-averaged value based on CFD results is within 2.3 percent for entire range of flow rate considered in this work. The fact that the predictions with the present model agree well with the area-averaged values rather than the mass-averaged values, implies that the present slip factor model can provide accurate prediction for absolute velocity in case with rather uniform distribution of flow within blade passage.

The correction method developed in this work is coupled with slip factor models to predict absolute circumferential velocities in Fig. 11. In comparison with Fig. 10, it is found that the predictions with the slip factor models are improved by the correction method, and thus become closer to the mass-averaged value rather than the area-averaged value except the case of Eck model. In most of the flow rate range, together with the correction method, Stodola and Wiesner models overestimate the mass-averaged absolute circumferential velocities slightly. The agreement between predictions and the CFD results are within 10.7 percent for Stodola model, and 5.6 percent for Wiesner model in entire range of flow rate

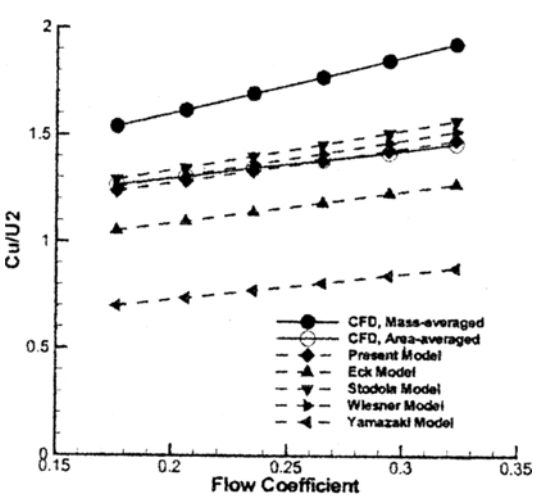

Fig. 10 Comparison of predicted circumferential-averaged velocity at exit of impeller

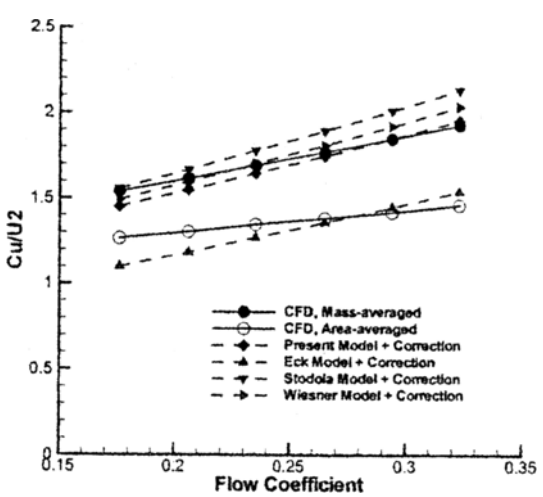

Fig. 11 Predicted $\bar{C}_{u2}$ at exit of impeller

range considered in this work. The mass-averaged absolute circumferential velocities predicted with the present slip factor model coupled with the present correction method are in reasonably good agreements with CFD results near and above the flow rate of peak total pressure coefficient (φ=0.265). However, at low flow rates, the accuracy of the prediction with the present model and correction method decreases (the relative error increases to 5.7 percent at φ=0.176). It implies that the effect of the large scale flow separation from suction surface induced by large incidence angle at low flow rate is not fully taken into account with the present correction method.

6. Conclusions

The slip factor model presented in this work for forward-curved blades centrifugal fan takes into account the effect of blade curvature. From the fact that the predictions with the present model agree well with the area-averaged slip factor and absolute circumferential velocity evaluated from the three-dimensional flow analysis results rather than with the mass-averaged values, it is suggested that the present slip factor model provides more accurate predictions for forward-curved centrifugal impeller with rather uniform flow within blade passage than the other slip factor models.

The reason why the slip factor models does not predict correctly the mass-averaged values is that the slip factor models do not take account of the viscous effects, i.e., the blockage effects in flow passage induced by the large scale backflow near the front plate and flow separation within blade passage due to large incidence angle. Thus, a correction method to take account of these blockage effects is also presented. The comparison with CFD results indicates that the correction method improves the results obtained with the slip factor models. The slip factor model presented in this work coupled with the present correction method provides accurate predictions for mass-averaged absolute circumferential velocity at the exit of impeller near and above the flow rate of peak total pressure coefficient, which is essential for the evaluation of theoretical total pressure rise.

References

Eck, B., 1973, "Fans," 1st ed., Pergamon Press, New York.

Kim, J. K. and Kang, S. H., 1997, "Effects of the Scroll on the Performance and Flow Field of a Sirocco Fan," ISROMAC-7, Hawaii, pp. 1318~1327.

Kind, R. J. and Tobin, M. G., 1990, "Flow in a Centrifugal Fan of the Squirrel-Cage Type," *ASME Journal of Turbomachinery*, Vol. 112, pp. 84~90.

Kind, R. J., 1997, "Prediction of Flow Behavior and Performance of Squirrel-Cage Centrifugal Fans Operating at Medium and High Flow Rates," *ASME Journal of Fluids Engineering*, Vol. 119, Sept., pp. 639~646.

Kwon, E. Y. and Cho, N. H., 2001, "Experimental Study on the Mean Flow Characteristics of Forward-Curved Centrifugal Fans," *KSME International Journal*, Vol. 15, No. 12, pp. 1728~1738.

Raj, D. and Swim, W. B., 1981, "Measurements of the Mean Flow Velocity and Velocity Fluctuations at the Exit of an FC Centrifugal Fan Rotor," *ASME Journal of Engineering for Power*, Vol. 103, April, pp. 393~399.

Sandra Velarde-Suarez et al., 1999, "Experimental Study on the Aeroacoustic Behavior of a Forward-Curved Blades Centrifugal Fan," *ASME Journal of Fluids Engineering*, Vol. 121, pp. 276~281.

Senoo, Y. et al, 1974, "Viscous Effects on Slip Factor of Centrifugal Blowers," ASME Journal of Engineering for Power, January, pp. 59~65.

Seo, S. J., Kim, K. Y. and Kang, S. H., 2003," Calculations of Three-Dimensional Viscous Flow in A Multi-Blade Centrifugal Fan by Modeling Blade Forces," Proceedings of The Institution of Mechanical Engineers, Part A-Journal of Power and Energy, Vol. 217, No. 3, pp. 287~298.

Stodola, A., 1927, "Steam and Gas Turbines,"

McGraw-Hill, New York.

Thomas Bouquet et al., 2002, "Study of the 3D Flows in the Forward-Curved Blades Centrifugal Fans," Proceedings of ASME 2002 Fluids Engineering Division Summer Meeting, Montreal, Quebec, Canada, July 14-18, 2002.

Wiesner, F. J., 1967, "Review of Slip Factors for Centrifugal Impellers," *ASME Journal of Engineering for Power*, Oct., pp. 558~572.

Yamazaki, S., 1986, "An Experimental Study on the Aerodynamic Performance of Multi-Blade Blowers (1st Report)," *Transactions of JSME (B)*, Vol. 52, No. 484, pp. 3987~3992.

Yamazaki, S., 1987a, "An Experimental Study on the Aerodynamic Performance of Multi-Blade Blowers (2nd Report)," *Transactions of JSME (B)*, Vol. 53, No. 485, pp. 108~113.

Yamazaki, S., 1987b, "An Experimental Study on the Aerodynamic Performance of Multi-Blade Blowers (3rd Report)," *Transactions of JSME (B)*, Vol. 53, No. 490, pp. 1730~1735.